Side-by-Side and End-to-End Gold Nanorod Assemblies for Environmental Toxin Sensing

ARTICLE *in* ANGEWANDTE CHEMIE INTERNATIONAL EDITION · JULY 2010

Impact Factor: 11.26 · DOI: 10.1002/anie.200907357 · Source: PubMed

9 AUTHORS, INCLUDING:

Wei Chen
Hefei University of Technology
193 PUBLICATIONS **5,148** CITATIONS
SEE PROFILE

Hua Kuang
Jiangnan University
155 PUBLICATIONS **2,073** CITATIONS
SEE PROFILE

Liqiang Liu
Jiangnan University
96 PUBLICATIONS **1,348** CITATIONS
SEE PROFILE

Nicholas Kotov
University of Michigan
445 PUBLICATIONS **26,694** CITATIONS
SEE PROFILE

Nanotechnology

DOI: 10.1002/ange.200907357

Side-by-Side and End-to-End Gold Nanorod Assemblies for Environmental Toxin Sensing**

Libing Wang, Yingyue Zhu, Liguang Xu, Wei Chen, Hua Kuang, Liqiang Liu, Ashish Agarwal, Chuanlai Xu, and Nicholas A. Kotov**

Controllable assembly of nanoscale building blocks (monomers) is a necessary part of practical realization of the unique optical, electrical, magnetic, and chemical properties of nanoscale matter in macroscale materials.[1–10] Such assemblies also contain much fundamental information about collective behavior of nanocolloids, which we are just beginning to understand.[11] The key decisive factors for the successful assembly of nanocolloids is the anisotropy of nanoscale interactions,[12,13] which stems from both the shape of nanocolloids[14–17] and unequal distribution of organic molecules on their surface.[18,19] Gold nanorods (Au NRs) have both geometrical and chemical anisotropy components[20] and demonstrate strong optical extinction in the range of visible and near-infrared (NIR) wavelengths convenient for both research and practical purposes.[21] Au NRs can be assembled by interactions with organic molecules,[22–24] polymers,[25,26] an antibody–antigen reaction,[27] biotin–streptavidin connectors,[28] and DNA,[29] leading to superstructures with different degree of organization and complexity of collective behavior.

Besides the utilization of NR monomers in non-linear optics,[28] cellular imaging,[30] and cancer therapy,[31] optical effects corresponding to monomer→superstructure transitions allowed preparation of excellent biosensors because of large changes in oscillation frequencies of plasmons when NR pairs are formed.[13,17,22] These studies mostly targeted biomedical applications. Simultaneously, their unique sensing capabilities have been virtually unexplored for the needs of environmental detection and monitoring.[28,29] These challenges and impact can equal or exceed those encountered in detection of cancer. A better understanding of methods for the realization of speed/selectivity/sensitivity detection of common environmental pollutants is thus of great importance.

Therefore, we decided to explore the potential of NR assemblies taking a pervasive environmental toxin, namely microcystin-LR (MC-LR), as the model while also addressing the general questions about the choice of different assembly motif for different sensing tasks. MC-LR is common in both developed and developing countries, with recorded cases of mass poisoning.[30,31] MC-LR originates from common blue-green algae and causes rapid liver failure;[32,33] prolonged exposure to small concentrations of MC-LR in drinking water causes liver cancer.[34] Herein, we describe the successful use of Au NRs for detection of MC-LR, which is significantly more sensitive than the traditional techniques, such as ELISA, yielding detection limit of 5 $pg\,mL^{-1}$. It is also much simpler and faster than any other methods.[35–38] These two factors are critical for environmental monitoring and have been a long-standing challenge. The pattern of the assembly strongly affects the sensitivity parameters for MC-LR detection.

To realize different modes of assembly, such as side-by-side and end-to-end motifs, with a degree of control sufficient for conclusive evaluation of sensing implications, two kinds of protein-carrying Au NRs were synthesized (Figure 1). One type of NR carried MC-LR antibodies (ABs) preferentially on the sides, while the other type carried antibodies located almost exclusively in the ends. These motifs were formed by using either electrostatic binding or covalent attachment of the antibodies mediated by a bifinctional linker, thioctic acid (TA). When electrostatic forces govern the placement of ABs, they attach primarily to the sides of NRs due to the larger area of contact and thus stronger electrostatic interactions. When a TA anchor covalently binds by a S−Au bond, the conjugation of the ABs occurs predominantly in the ends of the rods due to better accessibility of the gold surface to the reactive thiol end.[10,20,39,40] Variation of pH also allows varying repulsion or attraction of NRs and MC-LR, modality of attachment, and geometrical characteristics of assemblies (see the Supporting Information). The number of AB molecules on the surface of one Au NR was estimated to be 31 and 10 for the side-by-side

[*] L. Wang,[+] Y. Zhu,[+] L. Xu,[+] Dr. W. Chen,[+] H. Kuang, L. Liu, Prof. C. Xu
School of Food Science and Technology, State Key Laboratory of Food Science and Technology
Jiangnan University, Wuxi, 214122 (China)
E-mail: xcl@jiangnan.edu.cn
Dr. W. Chen,[+] A. Agarwal, Prof. N. A. Kotov
Department of Chemical Engineering, Department of Biomedical Engineering
Department of Materials Science and Engineering
University of Michigan, Ann Arbor, MI 48109 (USA)
E-mail: kotov@umich.edu
[+] These authors contributed equally to this paper.

[**] The authors thank the following institutions for support of this work: The National Science Foundation (NSF) (ECS-0601345, R8112-G1, 0932823, 0933384, 0938019), the Air Force Office of Scientific Research (AFOSR) (GRT00008581/RF60012388, 444286-P061716, FA9550-08-1-0382), the Department of Energy (DOE) EFRC program (DE-SC0000957), the National Natural Science Foundation of China (20675035, 20871060, 20835006), and the 11th Five Years Key Programs for Science and Technology Development of China (200810099, 200810219, 2008ZX08012-001).

Supporting information for this article, including details of nanorod synthesis, preparation of side-by-side and end-to-end assembles, ELISA tests that were performed, and instrumental analysis, is available on the WWW under http://dx.doi.org/10.1002/anie.200907357.

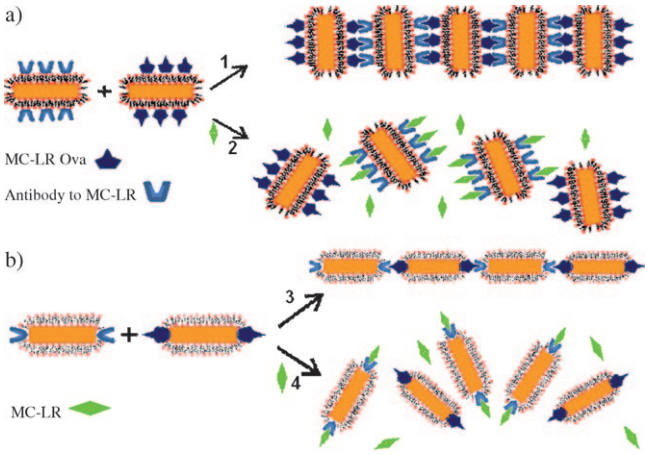

Figure 1. Toxin detection method with a) side-by-side and b) end-to-end nanorod assemblies. The numbers 1–4 denote routes for nanorod assembly.

and end-to-end motifs, respectively (see the Supporting Information).

To complement the Au NRs modified either in the end or in the sides with ABs, we also synthesized their analogues carrying MC-LR-OVA antigen. The same strategy to prepare the NRs modified by MC-LR-OVA on the sides and in the ends was used.

Transmission electron microscopy (TEM; Figure 2) indicated that side-modified complementary NR-MC-LR-OVA and NR-AB building blocks assemble in a distinct ladder pattern within 20 minutes. The combination of NRs with covalently bound ABs and NR-MC-LR-OVA in the ends gave nearly perfect chains in the same period of time (Figure 2), which is characteristic for most antibody–antigen immunocomplexes. Both NR patterns have certainly been observed in the past, but a high degree of control for each motif was still problematic.[21] Selective attachment of ABs makes possible the accurate manipulation of assembly geometries, including the distance between NRs.[26] It should also be mentioned that excellent stability of both ladder and chain superstructures was observed in aqueous dispersions for weeks.

Both motifs can be, in principle, used for MC-LR detection. With the increase of the MC-LR concentration in the solution, the toxin molecules compete with the MC-LP-OVA antigen immobilized on NRs. Therefore, progressively dominant presence of NR monomers is observed (Figure 2).

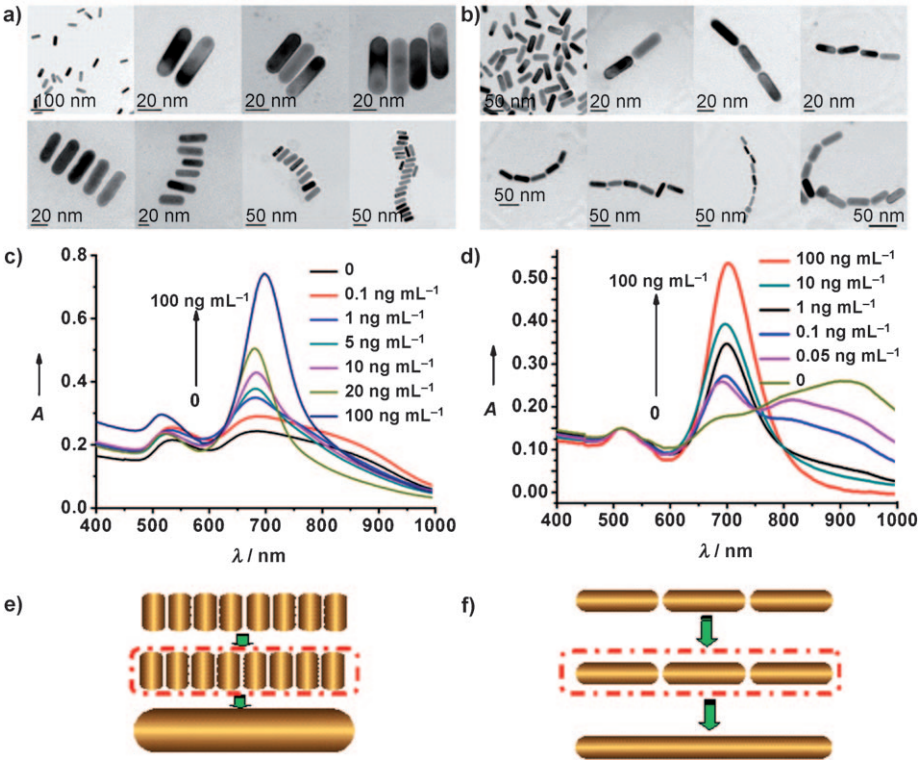

Figure 2. a,b) Representative TEM images for side-to-side and end-to-end nanorod assemblies. c,d) Evolution of surface plasmon resonance spectra of the nanorods upon increasing concentrations of microcystin-LR (MC-LR) indicated in the graph for side-to-side and end-to-end assemblies. e,f) Graphical representation of a plasmon system and corresponding nanowire approximation for side-to-side and end-to-end NR assemblies.

NR chains made from end-modified NRs can be approximated in terms of optical properties as nanowires (NWs),[41,42] which can be confirmed by the great similarity of their UV/Vis spectra.[43] The effect of MC-LR addition can thus be described as drastic reduction of a NW aspect ratio. The longitudinal surface plasmon peak of the newly formed much shorter rods shifted toward the blue part of the spectrum and increased in amplitude, while the transverse plasmon peak remained unchanged both in wavelength and amplitude. When the concentration of the MC-LR was 100 ng mL^{-1}, the original longitudinal peak at 900 nm almost disappeared and a new longitudinal peak at 700 nm appeared (monomers). The transverse plasmon peak did not change (Figure 2; Supporting Information, Figure S2) due to constancy of the diameter of the nanowire-like aggregates, whether they are assembled or not, which agrees with numerical simulation.[12,29] This observation also confirms that the transition of NR to chains and back does not involve any side-by-side assembly which would cause apparent "fattening" of the NRs. Similarly, with the increase of the MC-LR in the side-to-side assemblies, the longitudinal surface plasmon peak shifted to longer wavelength while the transverse peak shifted to shorter wavelength, indicating apparent "fattening" of the NRs.

Optical phenomena associated with the NR assembly transitions can be used as a powerful technique for environ-

mental monitoring of MC-LR. The protocol of competitive detection when NRs with two complementary coatings are added to the sample solution with MC-LR was used following the routes 2 and 4 in Figure 1. Calibration curves obtained for different MC-LR concentrations indicate that side-by-side and end-to-end assemblies give markedly different sensing parameters (Supporting Information, Figure S3). The detection range and the limit of detection (LOD) are 1–100 ng mL^{-1} and 0.6 ng mL^{-1} for the side-by-side mode; the corresponding sensing for the end-to-end mode are 0.05–1 ng mL^{-1} and 0.03 ng mL^{-1}. Improvements in excess of one order of magnitude for the end-to end assembly can be observed; a good correlation with the simple aspect ratio calculations should also be emphasized (Supporting Information, Figure S3).

Apart from UV/Vis absorption, other optical parameters can also be explored as the means for quantitative determination based on the NR assembly, for example the intensity of dynamic light scattering (DLS) at 633 nm, which can simplify environmental sensing.

The dramatic change of the aggregates size for MC-LR concentrations in both side-by-side and end-to-end types of assembly can be observed (Figure 3; Supporting Information, Figure S5). Importantly, in the range of small concentrations of MC-LR, the sensing plots for both types of assemblies registered by DLS have excellent linearity: from 0 to 100 ng mL^{-1} for the side-by-side assembly and from 0.01 to 25 ng mL^{-1} for the end-to-end assembly. Similar to UV/Vis data, the LOD are quite different in each case as well: 0.45 ng mL^{-1} and 5 pg/mL for the side-by side and end-to-end modes, respectively. Importantly, all results of the quantitative determination based on DLS are better than that of UV/Vis spectroscopy in both sensing range and LOD. Regarding the detection time, the advantage is also very obvious: The time of the developed method in both modes is just 15–20 min. This time can be compared with the time necessary to carry out is common ELISA testing including well preparation, that is, about 12 h. Overall, this constitutes a 36–48-fold time saving.

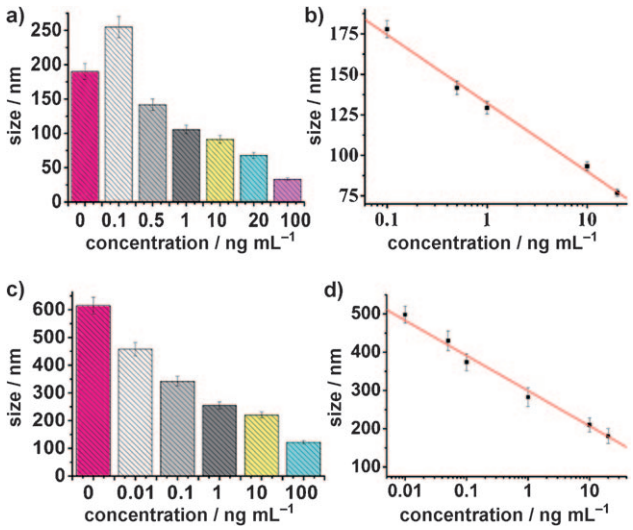

Figure 3. a) Hydrodynamic diameter of aggregates at different concentrations of MC-LR. b) Calibration curve for the side-by-side detection method. c) Hydrodynamic diameter of aggregates at different concentrations of MC-LR. d) Calibration curve for the end-to-end assembly detection method.

Considering the specificity, the developed method in end-to-end assembly modality was used to detect ochratoxin A while using the AB for MC-LR (Supporting Information, Figure S6). There is no cross-reactivity observed for the environmental target without direct complimentarity to produced AB. These results show specificity of the developed method.

The origin of markedly different sensing parameters in the two assembly motifs should be discussed, considering implications for the design of similar sensing systems for other environmental challenges. There are two mutually synergistic reasons for better LOD in case of end-to-end assembly: 1) Sensing parameters in UV/Vis spectroscopy are primarily dependent on the relative intensity of absorption of longitudinal plasmons in NRs versus assemblies; this difference is the most pronounced for end-to-end assemblies (Figure 2e–h).[12,44] For DLS detection the same considerations are applicable to aspect ratio and apparent hydrodynamic size. 2) The number of the ABs and MC-LR-OVA on the NR sides (Figure 1a) is much greater than that on the NR ends (Figure 1b). The same concentration of MC-LR has a much greater effect in the end-to-end structure than that in the side-by-side case.

In summary, MC-LR detection was successfully achieved with controllable assembly of Au NRs, which are modified either on the sides or ends, using covalent or electrostatic routes of protein attachment. The side-by-side and end-to-end assembly of the Au NRs were realized using complementary AB and antigen. Both sensitivity and detection ranges using UV/Vis spectroscopy and DLS are markedly better for the end-to-end motif. The sensing parameters for MC-LR using the NR assemblies surpass the required standard of drinking water by the World Health Organization (1 μg L^{-1}) and are substantially faster than existing methods. The controllable immunoassembly methods following the described approach can be applied to a large variety of environmental toxins by simple modification of the preparation procedure.

Received: December 31, 2009
Revised: May 14, 2010
Published online: July 2, 2010

Keywords: environmental monitoring · gold nanorods · microcystin · nanoscale assemblies

[1] R. D. Robinson, B. Sadtler, D. O. Demchenko, C. K. Erdonmez, L. W. Wang, A. P. Alivisatos, *Science* **2007**, *317*, 355–358.
[2] T. Mokari, E. Rothenberg, I. Popov, R. Costi, U. Banin, *Science* **2004**, *304*, 1787–1790.
[3] P. D. Cozzoli, T. Pellegrino, L. Manna, *Chem. Soc. Rev.* **2006**, *35*, 1195–1208.

[4] S. J. Hurst, E. K. Payne, L. D. Qin, C. A. Mirkin, *Angew. Chem.* **2006**, *118*, 2738 – 2759; *Angew. Chem. Int. Ed.* **2006**, *45*, 2672 – 2692.

[5] K. W. Kwon, M. Shim, *J. Am. Chem. Soc.* **2005**, *127*, 10269 – 10275.

[6] W. L. Shi, H. Zeng, Y. Sahoo, T. Y. Ohulchanskyy, Y. Ding, Z. L. Wang, M. Swihart, P. N. Prasad, *Nano Lett.* **2006**, *6*, 875 – 881.

[7] H. W. Gu, Z. M. Yang, J. H. Gao, C. K. Chang, B. Xu, *J. Am. Chem. Soc.* **2005**, *127*, 34 – 35.

[8] H. W. Gu, R. K. Zheng, X. X. Zhang, B. Xu, *J. Am. Chem. Soc.* **2004**, *126*, 5664 – 5665.

[9] Y. J. Min, M. Akbulut, K. Kristiansen, Y. Golan, K. Israelachvili, *Nat. Mater.* **2008**, *7*, 527 – 538.

[10] N. Zhao, K. Liu, J. Greener, Z. H. Nie, E. Kumacheva, *Nano Lett.* **2009**, *9*, 3077 – 3081.

[11] S. Srivastava, A. Santos, K. Critchley, K. S. Kim, P. Podsiadlo, K. Sun, J. Lee, C. Xu, G. D. Lilly, S. C. Glotzer, N. A. Kotov, *Science* **2010**, *327*, 1355 – 1359.

[12] Z. Y. Tang, N. A. Kotov, M. Giersig, *Science* **2002**, *297*, 237 – 240.

[13] P. Podsiadlo, A. K. Kaushik, E. M. Arruda, A. M. Waas, B. S. Shim, J. D. Xu, H. Nandivada, B. G. Pumplin, J. Lahann, A. Ramamoorthy, N. A. Kotov, *Science* **2007**, *318*, 80 – 83.

[14] C. J. Murphy, *ACS Nano* **2009**, *3*, 770 – 774.

[15] A. Sanchez-Iglesias, A. Grzelczak, M. R. Gonzalez, B. A. Puebla, R. A. Liz-Marzan, L. M. N. A. Kotov, *Langmuir* **2009**, *25*, 11431 – 11435.

[16] L. M. Liz-Marzán, *Langmuir* **2006**, *22*, 32 – 41.

[17] F. Kim, J. H. Song, P. D. Yang, *J. Am. Chem. Soc.* **2002**, *124*, 14316 – 14317.

[18] Y. Wang, T. Tang, X. Liang, L. M. Liz-Marzán, N. A. Kotov, *Nano Lett.* **2004**, *4*, 225 – 231.

[19] G. A. DeVries, M. Brunnbauer, Y. J. Hu, A. M. Long, B. Neltner, B. T. Uzun, O. Wunsch, B. H. Stellacci, *Science* **2007**, *315*, 358 – 361.

[20] Z. H. Nie, R. Daniele, M. Kumacheva, *J. Am. Chem. Soc.* **2008**, *130*, 3683 – 3689.

[21] P. J. Marek, J. Mulvaney, L. M. Paul, M. Luis, *Chem. Soc. Rev.* **2008**, *37*, 1783 – 1791.

[22] M. M. Kathryn, S. Y. Lee, H. W. Liao, B. C. Rostro, A. Fuentes, P. T. Scully, C. L. Nehl, J. H. Hafner, *ACS Nano* **2008**, *2*, 687 – 692.

[23] C. X. Yu, J. Irudayaraj, *Anal. Chem.* **2007**, *79*, 572 – 579.

[24] W. He, C. Z. Huang, Y. F. Li, J. P. Xie, R. G. Yang, P. F. Zhou, J. Wang, *Anal. Chem.* **2008**, *80*, 8424 – 8430.

[25] R. B. Grubbs, *Nat. Mater.* **2007**, *6*, 553 – 555.

[26] Z. H. Sun, W. H. Ni, Z. Yang, X. Kou, S. L. Li, J. F. Wang, *Small* **2008**, *4*, 1287 – 1292.

[27] J. Y. Chang, H. M. Wu, H. Chen, Y. C. Ling, W. H. Tan, *Chem. Commun.* **2005**, 1092 – 1094.

[28] H. Park, A. Agarwal, N. A. Kotov, O. D. Lavrentovich, *Langmuir* **2008**, *24*, 13833 – 13837.

[29] E. Dujardin, L. B. Hsin, C. R. C. Wang, S. Mann, *Chem. Commun.* **2001**, 1264 – 1265.

[30] G. V. Maltzahn, A. Centrone, J. H. Park, R. Ramanathan, M. J. Sailor, T. Hatton, A. S. N. Bhatia, *Adv. Mater.* **2009**, *21*, 1 – 6.

[31] J. L. Ferry, P. H. Craig, S. Cole, F. Patrick, P. Rebecca, L. F. Paul, H. S. Michael, I. G. Decho, A. W. Kashiwada, S. Murphy, J. Catherine, T. J. Shaw, *Nat. Nanotechnol.* **2009**, *4*, 441 – 444.

[32] A. K. Singh, D. Senapati, S. G. Wang, J. N. Griffin, C. Adria, N Perry, M. V. Khaleah, K. Birsen, *ACS Nano* **2009**, *3*, 1906 – 1912.

[33] G. Francis, *Nature* **1878**, *18*, 11 – 12.

[34] K. K. Caswell, J. N. Wilson, U. H. F. Bunz, C. J. Murphy, *J. Am. Chem. Soc.* **2003**, *125*, 13914 – 13915.

[35] L. B. Wang, W. Chen, D. H. Xu, B. S. Shim, Y. Y. Zhu, F. X. Sun, L. Q. Liu, C. F. Peng, Z. Y. Jin, C. L. Xu, N. A. Kotov, *Nano Lett.* **2009**, *9*, 4147 – 4152.

[36] S. B. Shim, W. Chen, C. Doty, C. L. Xu, N. A. Kotov, *Nano Lett.* **2008**, *8*, 4151 – 4157.

[37] W. Chen, C. F. Peng, Z. Y. Jin, R. R. Qiao, W. Y. Wang, S. F. Zhu, L. B. Wang, Q. H. Jin, C. L. Xu, *Biosens. Bioelectron.* **2009**, *24*, 2051 – 2056.

[38] W. Ma, W. Chen, R. R. Qiao, C. Y. Liu, C. H. Yang, Z. K. Li, D. H. Xu, C. F. Peng, Z. Y. Jin, C. L. Xu, S. F. Zhu, L. B. Wang, *Biosens. Bioelectron.* **2009**, *25*, 240 – 243.

[39] A. Agarwal, G. Lilly, A. Govorov, N. Kotov *J. Phys. Chem. C* **2008**, *112*, 18314 – 18320.

[40] P. Khanal, E. R. Zubarev, *Angew. Chem.* **2007**, *119*, 2245 – 2248; *Angew. Chem. Int. Ed.* **2007**, *46*, 2195 – 2198.

[41] J. M. Humphrey, J. B. Aggen, A. R. Chamberlin, *J. Am. Chem. Soc.* **1996**, *118*, 11759 – 11770.

[42] W. Wei, S. Li, L. D. Qin, C. Xue, J. E. Millstone, X. Y. Xu, G. C. Schatz, C. A. Mirkin, *Nano Lett.* **2008**, *8*, 3446 – 3449.

[43] S. Eustis, M. El-Sayed, *J. Phys. Chem. B* **2005**, *109*, 16350 – 16356.

[44] K. J. Prashant, E. Susie, M. A. El-Sayed, *J. Phys. Chem. B* **2006**, *110*, 18243 – 18253.

